Progress in Oceanography 224 (2024) 103248

Contents lists available at ScienceDirect

Progress in Oceanography

journal homepage: www.elsevier.com/locate/pocean

Spatio-temporal dynamics in microalgal communities in Arctic land-fast sea ice

Rebecca J. Duncan [a,b,*], Janne E. Søreide [b], Øystein Varpe [c,d], Józef Wiktor [e], Vanessa Pitusi [b,f], Elaine Runge [b,g], Katherina Petrou [a]

[a] School of Life Sciences, University of Technology Sydney, NSW, Australia
[b] Department of Arctic Biology, The University Centre in Svalbard, Longyearbyen, Norway
[c] Department of Biological Sciences, University of Bergen, Bergen, Norway
[d] Norwegian Institute for Nature Research, Bergen, Norway
[e] Institute of Oceanology, Polish Academy of Sciences, Sopot, Poland
[f] Department of Arctic and Marine Biology, University in Tromsø, Tromsø, Norway
[g] Department of Natural Sciences, University of Copenhagen, Copenhagen, Denmark

ARTICLE INFO

Keywords:
Sea ice microalgae
Svalbard
Nitzschia frigida
biogeochemical cycling
under ice light transmittance

ABSTRACT

Sea ice microalgae are an important source of energy for the polar marine food web, representing the primary carbon source prior to pelagic phytoplankton blooms. Here we investigate community dynamics of sea ice microalgal communities in land-fast sea ice across six different fjords in high-Arctic Svalbard, Norway, during Spring (April – May). We found that light (0.1 – 23% incoming PAR / 0.1 – 193 µmol photons $m^{-2}s^{-1}$) played a central role in determining community composition, with more diverse assemblages observed in sites with more light transmitted to the bottom ice community. In April, microalgal assemblages were similar when under-ice light transmittance was similar, independent of geographical location, however this light-derived separation of community structure was not evident in May. At all sites, assemblages were dominated by pennate diatoms, with the most abundant taxon being *Nitzschia frigida*. However, with increasing under-ice light transmittance, we saw an increase in the relative abundance of Dinophyceae, *Navicula* spp. and *Thalassiosira* spp.. A positive relationship between light and $\delta^{13}C$ enrichment and C:N ratios in the ice algal biomass demonstrated the effect of light on the biochemical composition of ice algae. Light did not correlate with cell abundance or chlorophyll *a* concentration. With anticipated changes to Arctic sea ice extent and snow cover as a result of climate change, we will see shifts in the light transmitted to the bottom ice community. These shifts, whether caused by reduced light transmittance from increased snow cover or increased light transmittance from thinning ice, snow depth or increased rainfall, will likely alter sea ice microalgal community composition, which in turn, may influence the success of secondary production and biogeochemical cycling in polar waters.

1. Introduction:

The sea ice-ocean interface forms a unique environment that provides a habitat for microalgae and micrograzers to live within a network of brine channels and tubes that exist on the bottom of the ice (Arrigo, 2014). This space-limited environment is characterised by sub-zero temperatures, changing nutrient availability, variable salinity and low light, frequently receiving < 10% incoming (incident) irradiance (Arrigo, 2014). The specialised photosynthetic sea ice biota that thrive in these dynamic physiochemical conditions are an important contribution to polar primary production. During spring, the biomass of the bottom ice assemblages can be up to ten times higher than for the adjacent seawater (Comeau et al., 2013; Michel et al., 1996), with values above 25 g C m^{-2} yr^{-1} often recorded (Smith et al., 1988). Thus, sea ice microalgal communities are an important source of energy for the polar marine food web (Kunisch et al., 2021; Michel et al., 1996).

The contribution of sea ice microalgae to primary production varies across time and space, ranging from 1 - 60% in ice-covered Arctic waters (Fernández-Méndez et al., 2015; Gosselin et al., 1997; Gradinger, 2009), and are a primary source of organic carbon for pelagic consumers in the early spring, extending biological production in polar waters by up to three months (Cota et al., 1991; Ji et al., 2013). In providing this initial

* Corresponding author at: University Technology Sydney, Building 7, 67 Thomas St, Ultimo, NSW Australia 2007.
E-mail address: rebecca.duncan@uts.edu.au (R.J. Duncan).

https://doi.org/10.1016/j.pocean.2024.103248
Received 6 April 2023; Received in revised form 8 February 2024; Accepted 24 March 2024
Available online 27 March 2024

food source during the early phases of seasonal zooplankton reproduction, sea ice algae play an important role in the quantity and quality of secondary production (Durbin & Casas, 2014; Leu et al., 2011; Søreide et al., 2010). In addition, sea ice algae are intricately linked with pelagic primary producers. With some taxa able to thrive in both the sympagic and pelagic environment, they may play a role in seeding the late spring /early summer pelagic phytoplankton blooms (Michel et al., 1993; Runge & Ingram, 1991; Tedesco et al., 2012). The sea ice algal cells not consumed in the water column, will often deposit on the sea floor and shallow littoral zone in a dormant or vegetative state, before being resuspended the following winter and spring (Vonnahme, 2021). In deeper areas, sea ice algal biomass is exported to depth where it is deposited on the ocean floor or remineralized (Boetius et al., 2013).

Diatoms (Bacillariophyceae) dominate sea ice algal communities (Arrigo, 2014; Hop et al., 2020; Horner, 1985). However, diversity within ice algal communities can vary from fewer than 20 taxa to over 150 taxa (Arrigo, 2014; Campbell et al., 2018; Hop et al., 2020), where the composition is controlled largely by species-specific responses to temperature, salinity, light, and nutrients (Campbell et al., 2018; Hop et al., 2020). For example, taxonomic diversity has been shown to increase with reduced sea ice thickness, related to a weakened dominance of *Nitzschia frigida* as the ice thins (Hegseth & von Quillfeldt, 2022). Similarly, centric diatoms can increase their relative abundance compared to pennate diatoms under higher light conditions (Campbell et al., 2018), whereas flagellates tend to outcompete diatoms when light is severely restricted (Rozanska et al., 2009). These dynamics in community composition affect carbon and nutrient cycling, as regulation of photosynthetic state (Kvernvik et al., 2021; Petrou & Ralph, 2011) and nutritional content are species specific in polar microalgae (Duncan et al., 2024; Duncan et al., 2022; Sackett et al., 2013). Furthermore, sea ice algal size structure influences nutrient uptake efficiency by primary consumers (Quetin & Ross, 1985) and nutrient supply and transfer to higher trophic levels (Hitchcock, 1982). Sea ice associated taxa are generally larger and more often chain-forming than open-oceanic phytoplankton (Arrigo, 2014). A community of larger cells in conjunction with the presence of aggregated chains, impacts the grazing efficiency due to micro- and mesozooplankton having a defined prey size range within which they can effectively graze (Berggreen et al., 1988; Quetin & Ross, 1985). In addition, in the early season when grazing pressure in the pelagic zone is minimal, the aggregated chains sink more quickly than single cells (Riebesell et al., 1991) to the ocean floor becoming an important food source for the benthos (McMahon et al., 2006). Taken together, community characteristics of size structure, nutritional content, growth rate and photosynthetic state are key to determining the extent to which the sea ice algae support the polar marine food web.

Thickness and areal coverage of land-fast ice has been declining rapidly for the past four decades across the Arctic (Yu et al., 2014) and in some areas, it has been reported to be declining at twice the rate of pack ice (Li et al., 2019). In Svalbard, land-fast ice extent in 2005-2019 was at 50% of the extent recorded in 1973-2000, with projections that the extent will decline to only 12% in the next 10-20 years (Urbański & Litwicka, 2022). In addition, the duration of sea ice coverage in Svalbard has reduced by up to four months since 2005 (Urbański & Litwicka, 2022), meaning the incorporation of sea ice assemblages into the ice is delayed and bloom termination and end of season ice melting occurs earlier. To understand the implications of such a decline in land-fast ice extent and duration on marine biodiversity and ecosystem function, it is important to understand how land-fast ice algal communities are affected by environmental change. To date, most studies into the composition of sea ice algal communities and their dynamics have focussed on pack ice communities. However, a handful of studies comparing algal communities between pack and land-fast ice (Archer et al., 1996; Comeau et al., 2013; Ratkova & Wassmann, 2005) found significant compositional differences between habitats, suggesting that our understanding of land-fast ice algal community dynamics is incomplete.

This study investigates the relationship between land-fast sea ice algal community composition and light transmissivity over the spring season (April-May) in Svalbard, Norway. Land-fast ice within six geographically distinct fjords was sampled to investigate spatial dynamics, while one fjord (Van Mijenfjorden) was sampled repeatedly throughout the spring to capture seasonality. The first hypothesis that is investigated is that sites with less snow cover and ice thickness, and therefore higher light transmissivity (higher under-ice light climate), would have a more abundant and taxonomically diverse algal community, with increased contributions of common pelagic taxa. The second hypothesis tested is that algal abundance and diversity would increase with the progression of spring until late spring, after which the advection of warmer waters would result in ice melt, attenuating community diversity and abundance.

1.1. Study Area

This study was conducted within six fjords in Svalbard, Norway (Fig. 1; Table S1) between April-May 2021. The sampling locations covered the west, north and east coasts of Spitsbergen; Van Mijenfjorden, Tempelfjorden, Billefjorden, Austfjorden, Agardhbukta and Inglefieldbukta. Whilst the sampling sites are relatively close by land access, they are not close oceanographically and are influenced by different water masses, meaning they are markedly different in their conditions. Van Mijenfjorden (70 km long and 10 km wide) is located on the south western coast. It is comprised of an inner basin with an approximate depth of 70 m and an outer basin approximately 120 m deep (Høyland, 2009). It is a partially enclosed fjord due to the presence of Akseløya island at the fjord mouth (Høyland, 2009), which minimises the advection of warm, saline Atlantic water transported to the area by the West Spitsbergen Current (WSC). The rather shallow and isolated fjord is efficiently cooled when air temperatures drop so the conditions are favourable for seasonal ice formation from January to June (Høyland, 2009). Tempelfjorden (14 km long and 5 km wide) is the innermost branch of Isfjorden, located in the central west coast and is divided into two basins; a smaller, glacial fed basin in the inner fjord up to 70 m deep and a central-outer basin up to 110 m deep (Forwick et al., 2010). Petuniabukta (6 km long and 3.5 km wide), is the innermost bay of another branch of Isfjorden - Billefjorden. A shallow sill prevents much of the advection of warm, Atlantic water penetrating the main area of Isfjorden, meaning sea ice cover generally persists from December-June in inner Billefjorden (Søreide et al., 2022). Austfjorden (35 km long and 5 km wide) is the innermost part of the 75 km long Wijdefjorden (totalling 110 km long), located on the north coast. The long, narrow nature of this fjord, and limited water exchange with offshore area due a cross-fjord sill, ensures reliable sea ice cover throughout January-May (Allaart et al., 2020). Inglefieldbukta (2.5 km wide bay) and Agardhbukta (8 km wide bay) are located on the south eastern coast of Spitsbergen and are exposed to cold Arctic water masses passing through adjacent Storfjorden. In addition, Inglefieldbukta receives glacial runoff from Inglefieldbreen. These sites have extensive snow and ice cover during December - July (Haarpaintner et al., 2001).

2. Materials & Methods

2.1. Sample Collection

Samples of sea ice algae were collected from the ice-water interface using a Kovacs core barrel (9 cm diameter; Kovacs Enterprise, USA). The bottom 3 cm of the sea ice was retained only (Smith et al., 1988). At each sampling site, six cores were taken approximately 1 m apart, with care taken to ensure the coring location was not disturbed. Cores were then pooled into triplicates, as cores 1-2, 3-4 and 5-6. Filtered seawater (100 ml of 0.7 μm GF/F) was added for each cm of core, to minimise osmotic stress (Campbell et al., 2019) and samples allowed to melt in darkness

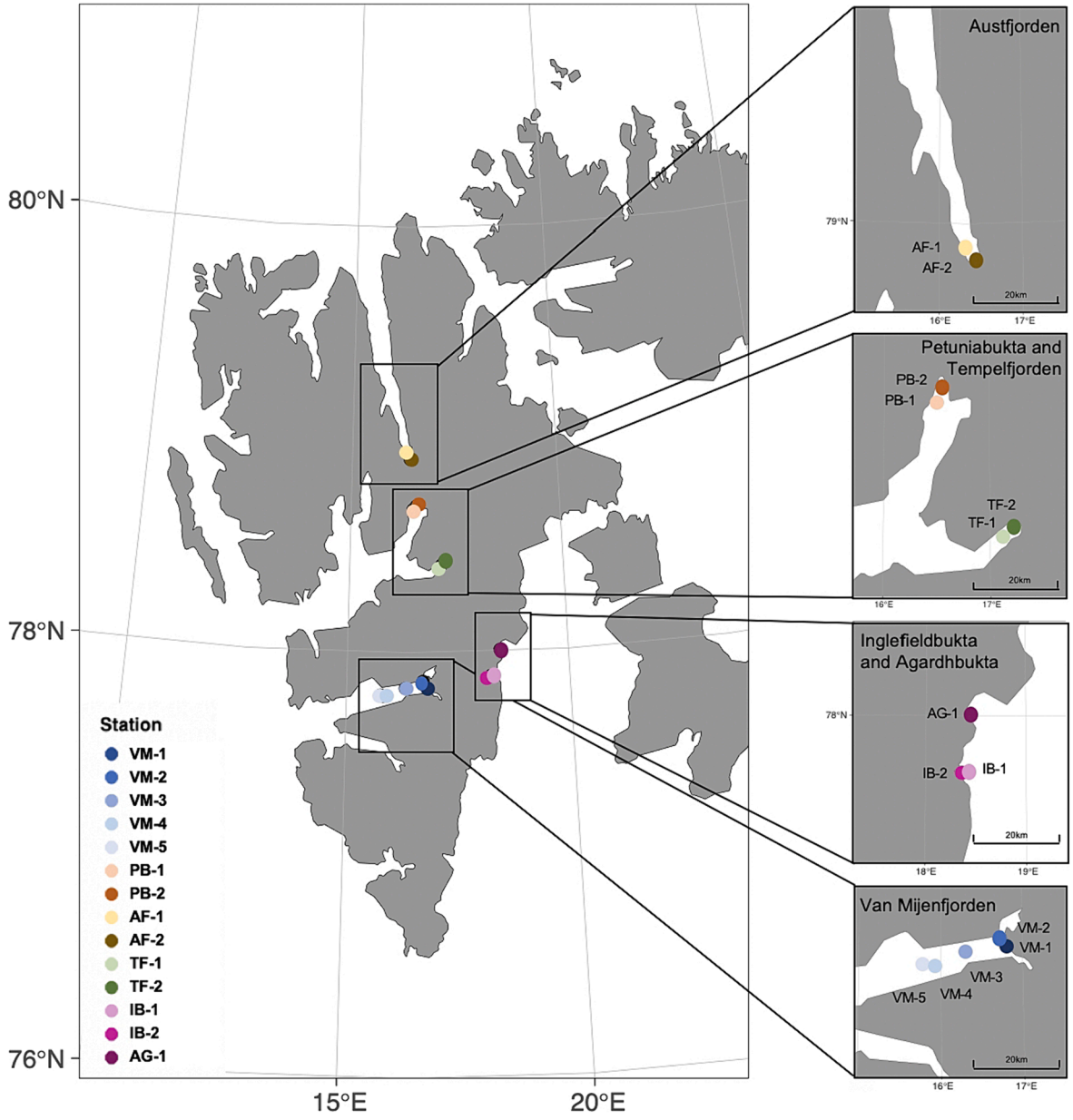

Fig. 1. Land-fast sea ice sampling locations visited between April- May 2021, within various fjords of Svalbard, Norway.

for 24 h at 4 °C. From each of the three pooled cores, subsamples of known volume were taken for determination of community composition, chlorophyll *a* (chl *a*) and particulate organic carbon and nitrogen (C:N). At each sampling event (date and station), under-ice water was collected using a 5L Niskin water sampler (KC Denmark, Silkeborg) and subsampled for chl *a,* particulate organic C:N and nutrient (nitrate plus nitrite ($NO_3^- + NO_2^-$), phosphate (PO_4^{3-}) and silicic acid ($Si(OH)_4$) and ammonium (NH_4^+)) analyses.

2.2. Physical Parameters

Prior to each core extraction, three snow depth measurements were taken using a standard ruler to determine snow depth in close vicinity to the planned core. Following core extraction, ice thickness was measured using a Kovacs ice thickness gauge (Kovacs Enterprise, Oregon, USA). Freeboard was measured at each core hole using a standard ruler. At each sampling event, two additional ice cores were taken to measure a salinity and temperature profile of the sea ice column. The temperature profile was measured *in situ*, in 10 cm intervals along the core. Following complete melting of separate 10 cm sections, salinity of each section was measured (Thermo Scientific Orion Versa Star Pro). At each sampling site, approximately 100 ml of the water collected from the ice-water interface was put into acid washed bottles and stored at -20 °C until nutrient analyses were performed. The $NO_3^- + NO_2^-$, PO_4^{3-}, $Si(OH)_4$ and NH_4^+ concentrations (μM/L) were measured simultaneously on a San++ 5000 automated analyzer (Skalar: Breda, Netherlands), with separate channels for the four nutrients. The detection limits were 0.02 μM/L for $NO_3^- + NO_2^-$, 0.01 μM/L for PO_4^{3-}, 0.25 μM/L for $Si(OH)_4$ and 0.3 μM/L for NH_4^+. At most sampling locations, a full temperature and salinity profile was measured of the water column below the ice using a CTD probe (STD/CTD SD204, SAIV A/S: Bergen, Norway). Brine salinity and volume were calculated according to (Cox & Weeks, 1983).

For the C:N and $\delta^{13}C$ and $\delta^{15}N$ stable isotope analysis, all six ice cores from each sampling point were pooled to obtain a minimum weight of 20 μg of N per filter, ensuring values were well above detection limits. Following complete melting, subsamples (300-1600 mL) of the ice cores and under-ice water (500-3000 mL) were filtered onto pre-combusted (400°C for 8h) filters (GF/F, 0.7 μm, Whatman). The filtration was

performed until visible colouration was observed and filters stored at -20°C until analysis (within 12 months). Filters were dried at 60 °C within sterile glass petri dishes, acid fumed (37% HCL for 8h), dried at 60 °C and placed into a tin cup. Samples were analysed at the Stable Isotope Facility at the University of California, Davis in an elemental analyser isotope ratio mass spectrometry (EA-IRMS) system, according to Barrie et al. (1989). The detection limits were 100 μg C for $\delta^{13}C$ and 20 μg N for $\delta^{15}N$.

2.3. Light Measurements and Modelling

At each sampling event, both incoming and transmitted photosynthetic active radiation (PAR) measurements were taken at the ice-ocean interface and snow-covered surface. For each measurement, a LI-190 quantum air corrected sensor was placed on the surface of the snow facing south. In the vicinity, a small hole was made using a 10 cm diameter auger, to lower a LI-192 underwater quantum sensor on a weighted frame, under the sea ice. To avoid shadowing of the measurement area, all sensors faced south with operations performed north, and the area was undisturbed. Measurements from both sensors were collected simultaneously using a LI-1500 Data Logger (LI-COR, Nebraska, USA). These measurements were then compared to modelled data (Table S2) using the equation:

Equation 1: $E_Z = E_0 \cdot \exp(-Kd \bullet Z)$

Where E_Z is irradiance at sampling depth Z (m), E_0 is the surface irradiance (μmol photons $m^{-2}s^{-1}$) and Kd is the diffuse light attenuation coefficient (m^{-1}). The PAR at the ice-ocean interface was estimated using *in-situ* measured irradiance at the top of snow and ice, and then attenuation through snow and ice was modelled using attenuation coefficients (Kd) of 20 m^{-1} for snow, 5 m^{-1} for the top 10 cm of ice, and 1 m^{-1} for ice below the top 10 cm (Perovich, 1996; Varpe et al., 2015).

To account for the fact that *in situ* measurements were taken at different times of day and with a range of cloud coverage conditions, percent incoming PAR was used as a proxy for under ice light at a given location, providing an estimate of the attenuation effects of the sea ice and snow depth at each site, as the differences in light conditions that the bottom ice algae communities were exposed to was determined primarily by the attenuating effects of snow depth and ice thickness. Because solar angle has a substantial effect on light quantity (Connan-McGinty et al., 2022) and cloud cover can reduce light intensity by up to 90% (Pfister et al., 2003), using percent incoming PAR allowed us to determine how effective ice and snow depth was at blocking incoming irradiance to the bottom ice community. This allowed us to utilise our unique *in situ* measurements, rather than a reliance on weather station data, which is either not available or not truly representative of the conditions in the fjords sampled. In this study, we therefore use light transmissivity to describe the percent incoming PAR under given snow and ice thicknesses.

2.4. Biological Parameters

2.4.1. Chlorophyll a content

Following complete melting, subsamples (60–450 mL) of each sea ice triplicate and a volume (500–2200 mL) of under-ice water were filtered (GF/F, 0.7 μm, Whatman, England). The filtration was performed until visible colouration of the filter and the filters were stored frozen (-80 °C) until extraction. Extractions were performed within three months of collection. Analyses were performed according to Holm-Hansen & Riemann (1978). Briefly, filters were extracted in 10 ml methanol and kept refrigerated for 24 h prior to extraction. Chl *a* content was measured with a calibrated 10-AU-005-CE fluorometer (Turner, California, USA), before and after acidifying the solution with 5% HCl (Parsons, 2013). For the sea ice samples, chl *a* content was converted to chl *a* biomass per unit ice surface area (mg/m^2).

2.4.2. Species Composition by Light Microscopy:

From each sampling site and date, subsamples (100 mL) were collected into a brown bottle and preserved with gluteraldehyde (2% final conc.). Between 4 and 10 mL (depending on cell density) of the well-mixed subsamples were poured into a 10 mL Utermöhl cylinder (KC Denmark, Silkeborg, Denmark) and the cells were allowed to settle for 6–24 h, depending on volume (Edler & Elbrächter, 2010). Cells were counted at 400x magnification and identified to lowest taxonomic level possible. The identification of species and groups was primarily based on the work of Tomas (1997) and Wiktor et al. (1995). It is unlikely that all pico- or nanoflagellates were captured. To ensure rare taxa were captured as much as possible, a whole chamber counting approach was employed. Qualitative and quantitative analyses were conducted under Nikon TS100 microscope, within 9 months of sample collection.

2.5. Data Analyses

To determine patterns in under ice community composition, similarity matrices were constructed using the Bray-Curtis coefficient on square root-transformed data (Somerfield et al., 2021) and visualised using non-metric multidimensional scaling (nMDS). The community composition of all sampled sites was contrasted between high light transmissivity (HLT) (>4% incoming PAR) and low light transmissivity (LLT) (< 3% incoming PAR) sites throughout the sampling period (14^{th} April 2021 – 25^{th} May 2021) by analysis of similarities (ANOSIM, Clarke & Warwick 1994), with the groupings established by ANOSIM, to determine if community composition was similar within similar light levels, independent of geographic location. The light groupings were determined based on the potential for photoinhibition in some ice-algal taxa beyond ~3% incoming PAR/ 20 μmol photons $m^{-2}s^{-1}$ (Palmisano et al., 1985; Ryan et al., 2011) and ensured sufficient replication for statistical comparison. To avoid temporal confounding between samples taken during different periods of the spring season while accounting for all sampling events, samples were divided into 'April' (14^{th} – 30^{th} April) and 'May' (4^{th} – 25^{th} May). The specific taxa contributing most to similarities/dissimilarities between the HLT and LLT sites were determined using similarity percentage analysis (SIMPER). To determine correlations between the community contribution of specific taxa, a correlation plot was created, using a correlation matrix of the percentage of community contribution of each taxon.

To establish relationships between percentage contribution to community composition of taxonomic groups (Fig. 2-3) and percent incoming PAR, a linear regression (95% confidence interval) was applied to each taxonomic group, including all sampling events. In cases in which the data were poorly explained by a linear fit, a second order polynomial regression was applied. The Shapiro–Wilks (Shapiro & Wilk, 1965) test for normality showed that the modelled light and cell density data required $\log_{10}$ transformation before analysis. Regressions were tested for overall model significance using the *F* statistic ($P < 0.05$) and strength of fit using R^2. The residuals of all regressions were verified for homoscedasticity. Differences in cell density between HLT and LLT sampling sites in April and in May were determined using PERMANOVA. Differences between C:N and stable isotopes of organic carbon and nitrogen between HLT and LLT sites were determined using a Welch t-test. To investigate which environmental variables account for a significant difference in the species composition, redundancy analysis (RDA) was performed, constrained to environmental variables ($n = 15$) with Monte Carlo permutations (999), and only significant vectors are displayed. The percent incoming PAR levels used throughout all statistical analyses were taken from the modelled light, to ensure consistency and avoid any data gaps. All analyses were performed using RStudio v. 2022.02.03 (R Core Team, 2022) and the add-on packages 'vegan' v.2.5-7 (Oksanen et al., 2013), 'ggplot2' v.3.3.6 (Wickham et al., 2016) and 'dplyr' v.1.0.8 (Wickham et al., 2019).

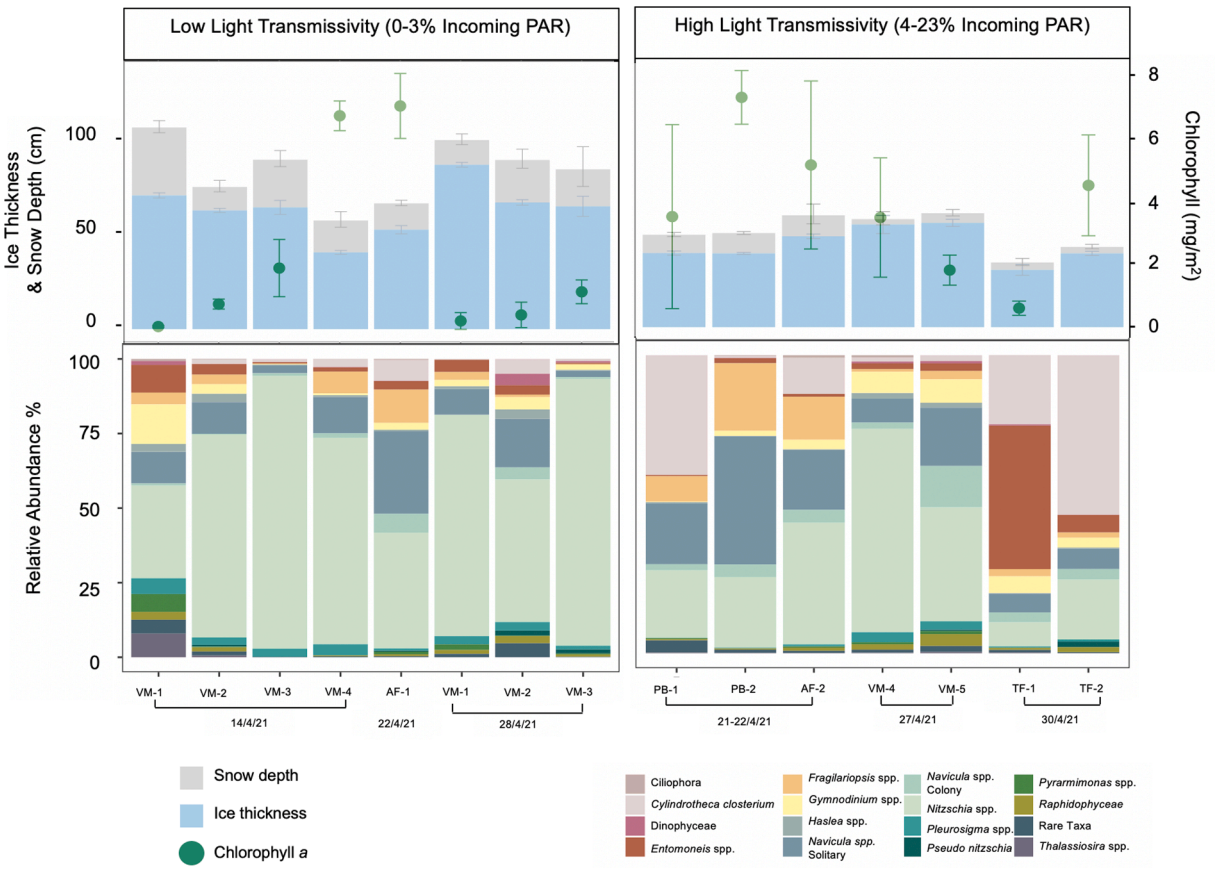

Fig. 2. Bottom ice microalgal community composition from low light transmissivity (left) and high light transmissivity (right) sites sampled during April 2021, in Svalbard, Norway. Snow depth (grey), ice thickness (blue), and chlorophyll *a* content (mg/m^2) (green circles) are displayed in the upper panels +/- SD (n = 18, n = 6 and n = 3, respectively), relative abundance (%) of taxonomic groups are shown in the lower panels.

3. Results

3.1. Physical Characteristics

Across all sampling sites, sea ice thickness ranged from 30–104 cm (Table 1) and snow depth from 3–36 cm (Table 1; Fig. 2-3). The temperature of the bottom 3 cm of ice (at the ice-water interface) ranged from -1.9 to -3.6 °C (Table 1), and bulk ice salinity from 1.7–10.7 ppt (Table 1). The brine salinity ranged from 33.9–62.8 ppt (Table 1) and the brine volume ranged from 3.4–25.4 % ice volume (Table 1). Water temperature and salinity varied only minimally across all sites, with temperature ranging from -1.4 °C to -1.9 °C and salinity ranging from 33–34.5 ppt (Table S3). At all sites, the seawater was nutrient replete, with mean $NO_3^- + NO_2^-$, PO_4^{3-} and $Si(OH)_4$ concentrations of 2.01 +/- 0.5 μM, 2.01 +/- 0.3 μM, and 0.21 +/- 0.0 μM, respectively, and NH_4^+ levels generally <1 μM (Table S3).

3.2. Chlorophyll a, carbon and nitrogen:

Bottom ice chl *a* ranged from 0.15–7.2 mg/m^2 (Table 1; Fig. 2-3), while chl *a* in the water column directly below the sea ice ranged from 0.04–1.94 mg /m^3 (Table S3). We observed a positive relationship between cell density and chl *a* ($F_{1,28} = 28.68$, $p > 0.05$; $R^2 = 0.51$), but we found no relationship between under-ice light transmissivity and bottom ice chl *a* ($F_{1,28} = 0.00$, $p > 0.05$; $R^2 = 0.00$) or water column chl *a* ($F_{1,28} = 3.20$, $p > 0.05$; $R^2 = 0.10$).

Molar ratios of C:N ranged from 4.53–13.80 in samples taken of the sea ice (Table 1) and 2.24–13.20 in under-ice water (Table S3). The C:N ratio was significantly higher in the sea ice at HLT compared to LLT sites in April ($t(7) = 2.5$, $p < 0.05$), but did not differ in May ($t(5) = 1.31$, $p > 0.05$). We found no difference in under-ice water C:N between HLT and LLT sites in either April or May.

Sea ice stable isotope of organic carbon ($\delta^{13}C_{VPDB}$) ranged from to -27.05 to -14.34 ‰ (Table 1) and organic nitrogen ($\delta^{15}N_{Air}$) ranged from 1.92–6.34 ‰ (Table 1). Under-ice water $\delta^{13}C$ ranged from -24.99 to -28.41 ‰ (Table S2) and $\delta^{15}N$ ranged from 1.68 to 8.54 ‰ (Table S3). The samples taken from the sea ice at HLT sites were significantly more carbon enriched than those taken from the LLT sites in April ($t(7) = 3.5$, $p < 0.05$) and in May ($t(5) = 2.95$, $p < 0.05$). We found a positive correlation between under-ice light and $\delta^{13}C$ throughout April and May ($F_{1,28} = 23.96$, $p < 0.05$; $R^2 = 0.46$), however no correlation was detected between $\delta^{13}C$ values and cell density or chl *a*. There was no difference in nitrogen enrichment between HLT and LLT sites in April ($t(8) = -2.56$, $p > 0.05$), however the LLT sites did have higher nitrogen enrichment in May ($t(10) = -2.45$, $p < 0.05$). A negative correlation was observed between $\delta^{15}N$ values and cell density ($F_{1,28} = 30.59$, $p < 0.05$; $R^2 = 0.52$) and $\delta^{15}N$ values and chl *a* ($F_{1,28} = 28.54$, $p < 0.05$; $R^2 = 0.50$), but no correlation was detected between $\delta^{15}N$ values and under-ice light. Unlike $\delta^{13}C$ values, $\delta^{15}N$ increased as the season progressed ($F_{1,28} = 7.27$, $p < 0.05$; $R^2 = 0.21$). There was no difference in carbon or nitrogen enrichment in under-ice water between HLT and LLT in either April or May.

3.3. Under-ice Light Transmissivity

Measured percent incoming PAR varied from 0.02–6.10 % (0.1–50 μmol photons m^{-2}s^{-1}) across 21 of 30 sites and dates, and measured surface irradiance varied from 387–1314 μmol photons m^{-2}s^{-1}. Modelled percent incoming PAR varied from 0.02–23.18% incoming PAR (0.1–193, $\bar{X} = 35 \pm 52$ μmol photons m^{-2}s^{-1}) across all 30 sites and

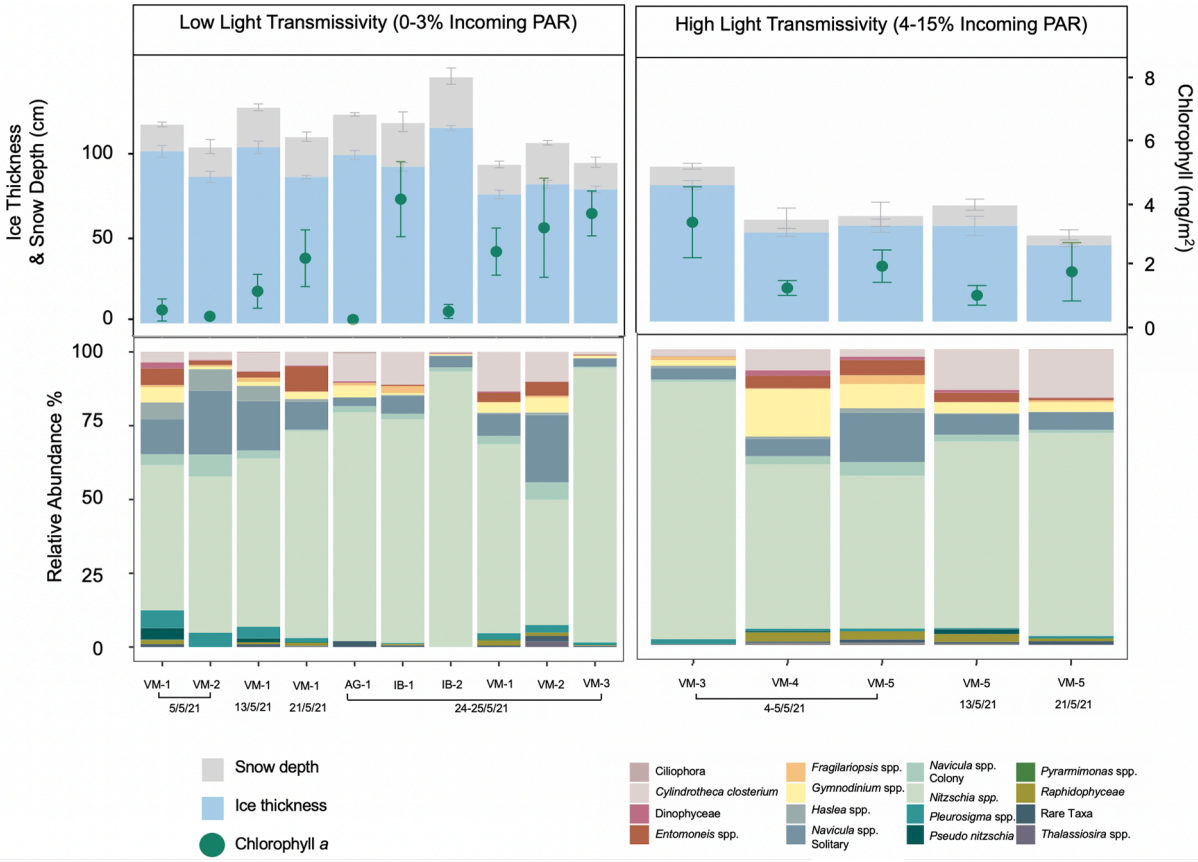

Fig. 3. Bottom ice microalgal community composition from low light transmissivity (left) and high light transmissivity (right) sites sampled during May 2021, in Svalbard, Norway. Snow depth (grey), ice thickness (blue), and chlorophyll *a* content (mg/m^2) (green circles) are displayed in the upper panels +/- SD (n = 18, n = 6 and n = 3, respectively), relative abundance (%) of taxonomic groups are shown in the lower panels.

times (Table S2; Fig. 2–3). Based on the average incoming irradiance of 750 µmol photons m^{-2}s^{-1}, the percentage of light transmitted equates to a range of 0.1–204 µmol photons m^{-2}s^{-1} transmitted to the bottom ice community. For the locations where *in situ* light measurements were obtained (21 out of 30), these values closely resembled the modelled light measurements, with the modelled light values slightly higher +1.25% (+/- 3.21%) on average, than the measured light levels (Table S2). The total variance in the modelled % incoming PAR was -4.7 to 10.3%. When plotted against each other, the modelled and measured values were significantly correlated ($r_{19} = 0.5$, $p < 0.05$).

3.4. Species Composition

We identified a total of 55 taxa (to species or genus level), corresponding to seven phylogenetically distinct groups, with Bacillariophyceae accounting for 42 species (76% of the total), Dinophyceae accounting for six species (11%) and Pyramimonadophyceae being represented by three species (5%) (Table S4–S5). Raphidophyceae, Cryptophyceae, Euglenoidea and Ciliophora were identified to class level only. Of the identified diatoms, 40 species (95%) were from the order Pennales, while only two species belonged to the Centrales (5%). At all sites, the community was dominated by *Nitzschia* spp. (Figs. 2–3; Table 1). The *Nitzschia* spp. group, while dominated by colonial *N. frigida,* was represented also by colonial *N. promare, N. arctica, N. laevissima, N. brebissoni,* and *N. polaris.* Similarly, for the solitary *Navicula* group, *N. directa* was the most common and abundant, however, *N. distans, N. kariana, N. transitas, N. algida, N. valida* and *N. pellucida* were also present. The colony forming (ribbon) *Navicula* group consisted of *N. pelagica, N. septentrionalis, N. granii* and *N. vanhoefenii.* The Dinophyceae group was primarily identified to class level but also included *Peridiniella catenata* and *Peridiniella* spp.. *Gymnodinium* spp. was not included in the Dinophyceae group as it was included as a separate grouping at genus level. The *Fragilariopsis* spp. group was dominated by *Fragilariopsis cylindrus* but included *F. reginae-jahniae* and *F. oceania.* The *Thalassiosira* spp. group was primarily identified to genus level but included *T. nordenskioeldii.* The 'Rare Taxa' group included euglenophytes, uncommon diatom taxa and haptophytes (Table S4).

While *Nitzschia* spp. dominated the communities during April–May from both the HLT and LLT sites, there were clear shifts in percentage contribution of scarcer taxa with increased irradiance. For example, *Cylindrotheca closterium* and colony forming *Navicula* spp. became more prominent when incoming PAR was >4% during April (Figs. 2–3). In addition, throughout April, *Entomoneis* spp. was generally found in higher relative abundance in the LLT sites, with the exception of TF-1 where it was found to be the dominant taxa (Fig. 2). During May, *Gymnodinium* spp. tended to have a higher relative abundance at sites with HLT (Fig. 3).

3.5. Influence of Light Transmissivity on Protist Community Composition

Spatial and temporal differences, associated with differing under-ice light climates, related to community composition during April, but not during May (Fig. 4a–b). When compared, HLT sites differed in community composition from the LLT sites during April (ANOSIM R = 0.26, $p < 0.05$; Fig. 2), with the LLT (< 3% incoming PAR / < 20 µmol photons m^{-2}s^{-1}) generally dominated by *Nitzschia* spp. (primarily *N. frigida),* compared to a more diverse community in the high light sites (> 4% incoming PAR / > 21 µmol photons m^{-2}s^{-1}) with an increased contribution of various *Navicula* spp., *C. closterium* and *Fragilariopsis* spp. (Fig. 2). The cumulative contribution to this dissimilarity between HLT

Table 1
Parameters measured associated with sea ice core extraction; snow depth (+/- SD, n = 18), ice thickness (+/- SD, n = 6) and within the bottom 3cm of sea ice core; salinity (ppt), brine salinity (ppt), brine volume (% of ice volume), chlorophyll *a* concentration (mg/m^2) (n = 3), daylight hours at time of sampling, carbon:nitrogen (C:N) ratio, carbon isotope ratio ($\delta^{13}C_{VPDB}$ (‰)) and nitrogen isotope ratio ($\delta^{15}N_{Air}$ (‰)).

Date	Station	Snow Depth (cm)	Ice Thickness (cm)	Ice Temperature (°C)	Salinity (ppt)	Brine Salinity (ppt)	Brine Volume (% ice volume)	Chlorophyll *a* (mg/m^2)	Daylight (Hours)	C:N	$\delta^{13}C$ (‰)	$\delta^{15}N$ (‰)
14.4.21	VM-1	36.4 +/- 1.9	72 +/- 1.4	-2.3	8.6	40.77	18.85	0.15+/-0.0	15.09	4.61	-25.61	5.28
14.4.21	VM-2	12.6 +/- 1.8	64 +/- 1.1	-2.5	8.9	44.16	17.99	0.86+/-0.16	15.09	4.69	-24.68	4.57
14.4.21	VM-3	25.5 +/- 2.5	65 +/- 3.8	-3.6	9.8	62.38	13.91	1.98+/-0.90	15.09	5.51	-25.09	3.14
14.4.21	VM-4	16.9 +/- 2.4	41 +/- 1.0	-2.5	1.7	44.16	3.44	6.74+/-0.46	15.09	4.65	-24.29	1.92
21.4.21	PB-2	9.5 +/- 0.6	39 +/- 1.1	-2.3	4.7	40.77	10.30	3.49 +/2.89	19.55	5.50	-24.37	3.56
21.4.21	PB-3	10.6 +/- 0.4	38 +/- 0.5	-2.3	4.7	40.77	10.30	7.24+/-0.85	19.55	6.53	-18.82	3.64
22.4.21	AF-1	14.16 +/-0.8	53 +/- 2.2	-2.3	7.2	40.77	15.78	7.05+/1.02	19.59	5.28	-24.22	3.41
22.4.21	AF-2	10.9 +/-2.9	47 +/- 1.2	-2.7	3.8	47.53	7.13	5.11+/-2.64	19.59	5.64	-23.25	4.07
27.4.21	VM-4	2.8 +/-2.0	54 +/-4.7	-2	9.6	35.64	24.12	3.46+/-1.88	20.36	7.19	-18.08	3.73
27.4.21	VM-5	5.0 +/-1.0	54 +/-1.9	-2.1	10.6	37.36	25.39	1.80+/-0.47	20.36	4.99	-22.97	3.79
28.4.21	VM-1	13.2 +/-1.7	88 +/-1.3	-2	9.2	35.64	23.12	0.33+/-0.26	20.36	4.53	-24.73	5.75
28.4.21	VM-2	22.7 +/-2.9	68 +/-1.5	-2.1	9.6	37.36	23.00	1.24+/-0.40	20.36	5.96	-24.43	5.32
28.4.21	VM-3	19.8+/- 6.1	66 +/-5.4	-2.2	3.2	39.07	7.33	1.36+/-0.35	20.36	5.26	-26.88	3.35
30.4.21	TF-1	3.9 +/-1.1	30 +/-2.8	-2.2	3.2	39.07	7.33	0.61+/-0.22	20.47	7.52	-14.34	4.39
30.4.21	TF-2	3.4 +/-0.7	38 +/-1.1	-2.7	9.2	47.53	17.25	4.47+/-1.59	20.47	10.18	-15.90	4.57
4.5.21	VM-3	10.0 +/-0.9	74 +/-2.6	-2.2	10.4	39.07	23.81	3.11+/-1.13	21.05	6.02	-25.27	3.42
4.5.21	VM-4	7.0 +/-3.2	50 +/-2.2	-2.1	5.6	37.36	13.42	1.01+/-0.24	21.05	7.50	-21.05	4.73
4.5.21	VM-5	4.8 +/-3.8	52 +/-3.6	-2.2	6.2	39.07	12.82	1.70+/-0.52	21.05	6.92	-15.31	3.04
5.5.21	VM-1	14.3 +/-0.7	92 +/-3.2	-2.1	6.5	37.36	15.57	0.55+/-0.35	21.05	6.09	-24.99	6.34
5.5.21	VM-2	15.8 +/-2.1	78 +/-3.0	-2.2	10.7	39.07	24.49	0.35+/-0.07	21.05	5.73	-24.30	5.31
13.5.21	VM-1	21.2 +/-1.0	94 +/-3.3	-2.1	9.5	37.36	22.76	1.14+/-0.53	24	7.57	-24.64	4.49
13.5.21	VM-5	11.0 +/-1.7	52 +/-5.2	-2	ND	ND	ND	0.77+/-0.31	24	10.99	-17.13	4.41
21.5.21	VM-1	21.2 +/-1.4	78 +/-0.9	-2	7.9	35.64	19.85	2.18+/-0.90	24	5.83	-24.61	5.06
21.5.21	VM-5	5.3 +/-1.6	42 +/-0.7	-2	ND	ND	ND	1.52+/-0.93	24	13.80	-15.90	4.65
24.5.21	AG-1	21.7 +/-0.5	90 +/-2.5	-2.5	5	44.16	10.10	0.25+/-0.10	24	11.15	-27.05	6.27
24.5.21	IB-1	23.5 +/-3.0	84 +/-2.3	-1.9	9.2	33.92	24.31	4.04+/-1.18	24	6.02	-26.74	3.48
24.5.21	IB-2	26.5 +/-2.5	107 +/-1.3	-1.9	6.6	33.92	17.44	0.50+/-0.22	24	5.54	-24.98	6.29
25.5.21	VM-1	15.9 +/-1.0	70 +/-2.3	-2	7.9	35.64	19.85	2.39+/-0.74	24	7.13	-23.09	5.24
25.5.21	VM-2	22.1 +/-0.7	75 +/-2.1	-2	7.4	35.64	18.59	3.14+/-1.56	24	6.48	-24.20	5.42
25.5.21	VM-3	14.2 +/-1.6	72 +/-1.7	-2	9.5	35.64	23.87	3.59+/-0.71	24	8.54	-21.84	3.96

ND represents measurement not taken.

and LLT sites was from *Nitzschia* spp. (11%), *C. closterium* (21%) *N. transitas* (27%), *F. cylindrus* (31%), *N. septentrionalis* (35%), *F. oceania* (39%), *Entomoneis* spp. (43%), *P. taeniata* (47%) and *Gymnodinium spp.* <10μm (50%). In May, however, the HLT and LLT assemblages were similar, indicating that community composition was similar irrespective of light climate, sampling location or sampling date (2D Stress = 0.16, Fig. 4b). In May, the community composition of both HLT and LLT sites (ANOSIM R = 0.00, p > 0.05; Fig. 3) were dominated by *Nitzschia* spp., specifically, *N. frigida* (Fig. 3).

At an individual species level, we found significant relationships between the relative abundance and light transmissivity for five taxa (Fig. 5). For the most predominant species, *N. frigida,* the percentage contribution to the community decreased as light transmissivity increased ($F_{1,28} = 6.30$, $p < 0.05$; $R^2 = 0.18$). In contrast, for the other four taxa, *Gymnodinium* spp. ($F_{1,26} = 13.77$, $p < 0.05$; $R^2 = 0.35$), colony-forming *Navicula* spp. ($F_{1,23} = 11.36$, $p < 0.05$; $R^2 = 0.33$), Dinophyceae ($F_{1,27} = 6.58$, $p < 0.05$; $R^2 = 0.20$) and *Thalassiosira* spp. ($F_{1,24} = 14.05$, $p < 0.05$; $R^2 = 0.37$), their percentage contribution to the community increased as under-ice light transmissivity increased. No trend between under ice light and contribution to the community was found for the other taxonomic groups (Table S6).

During April and May, we detected patterns in species occurrences. While there was a consistently negative correlation between *Nitzschia* spp. and all other taxa (Fig. 6a), we did detect strong positive correlations between the presence of *Thalassiosira* spp., *Raphidophyceae* spp. and *Pyramimonas* spp., high co-occurrence of *Pleurosigma* spp. and

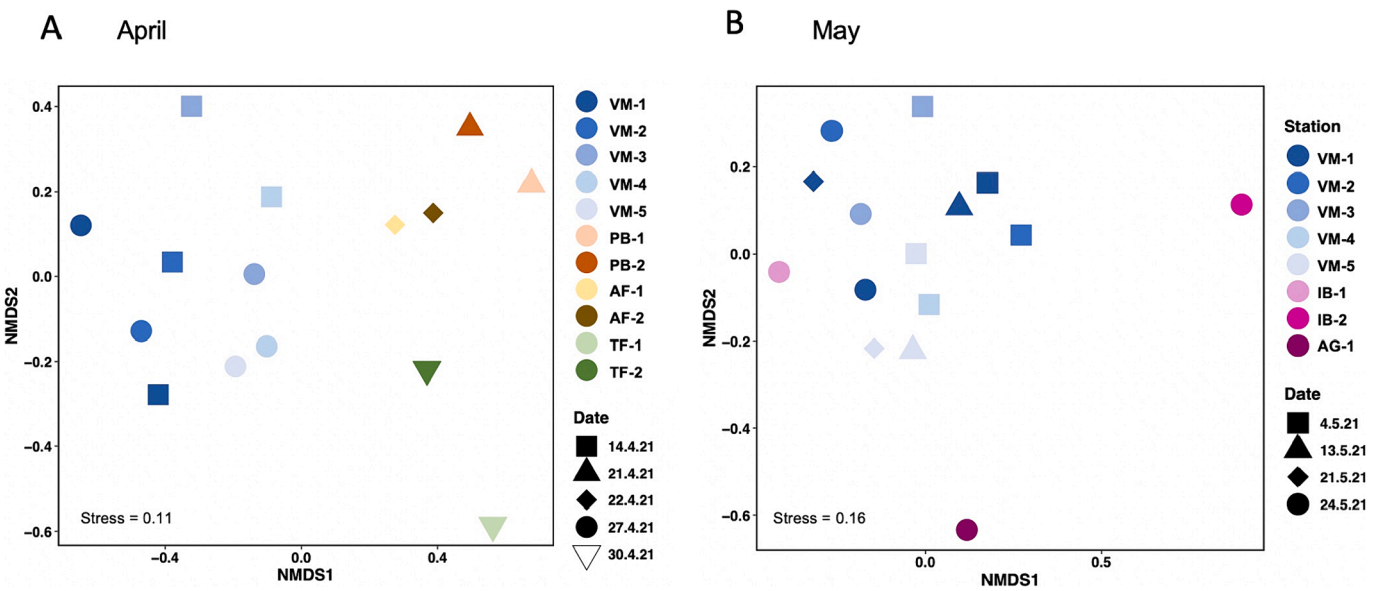

Fig. 4. Non-metric multidimensional scaling (nMDS) of microalgal communities for (A) April and (B) May, based on resemblance using Bray-Curtis similarity. Sample sites are shown by colour and dates by shapes. The 2D stress is shown in the lower left.

Haslea spp., as well as high co-occurrence of *Fragilariopsis* spp. with solitary *Navicula* spp. (Fig. 6a). Environmental conditions explained 58.7% (on two canonical axes) of the variability in community composition ($F_{15} = 3.37$, $p < 0.05$, Fig. 6b). Abundance of *N. frigida* and *Thalassiosira* spp. was most strongly associated with chl *a* concentration, whilst the prevalence of *Entomoneis* spp., *C. closterium*, *Navicula* spp. (solitary and colony forming), *Gymnodinium* spp. and *Fragilariopsis* spp. was explained by percent incoming PAR more than any other variable (Fig. 6b). Brine salinity was the most explanatory variable for the presence of *Pleurosigma* spp., while the contribution from Dinophyceae appeared to be linked to $\delta^{15}N$ (Fig. 6b).

3.6. Relationships between light transmissivity and community diversity

Accounting for all sampling events across time and space (both April and May), sea ice algal species diversity increased with increasing percent incoming PAR ($F_{1,28} = 4.6$, $p < 0.05$; $R^2 = 0.14$; Fig. 7a). However, we detected a decline in diversity from April to May. Using the five-time repeated transect from the outermost (VM-5) to the innermost (VM-1) part of Van Mijenfjorden (Fig. 1), we found that diversity at the outer site (VM-5) declined significantly through time ($F_{1,2} = 29.17$, $p < 0.05$; $R^2 = 0.94$; Fig. 7b) as did the inner site (VM-1), with a sharp dip on the 27th April ($F_{1,3} = 28.03$, $p < 0.05$; $R^2 = 0.90$; Fig. 7b). Interestingly, this temporal decline in diversity was independent of light transmissivity and the changes that resulted in lower diversity differed between sites. As time progressed, the community at the VM-5 site had an increase in the relative abundance of *N. frigida* and *C. closterium* concurrent with a decrease in *Gymnodinium* spp., *Haslea* spp., *Fragilariopsis* spp. and *Navicula* spp. In contrast, the community at VM-1 saw an increase in *N. frigida* and *C. closterium,* with a decline in *Gymnodinium* spp. and *Pleurosigma* spp. as the season progressed. Whilst light transmissivity was not linked to the diversity index within sites, light transmissivity likely influenced the differences in community composition between the two sites (ANOSIM R: 0.28, $p < 0.05$), as the sampling sites within Van Mijenfjorden differed in modelled percent incoming PAR during the sampling period (ANOVA: $F_{4,14} = 3.63$, $p < 0.05$), with the greatest difference observed between VM-1 and VM-5 sites (Tukey's HSD: $p < 0.05$, 95% CI = [-0.04 – 3.53]). No relationship was found between cell density and percent incoming PAR ($F_{1,28} = 4.27$, $p > 0.05$; $R^2 = 0.13$).

4. Discussion

In this study, we investigated bottom ice microalgal community composition in land-fast sea ice at both temporal and spatial scales. We evaluated under-ice light using a light transmittance model based on the physical parameters of ice thickness and snow depth. Validating against our *in situ* measurements, we found that modelled results were in good agreement with measured values and were thereby used to avoid the variability inherent in obtaining light data *in situ* that is complicated by time of day or variable weather conditions. Whilst it is difficult to directly compare under-ice light measurements with those measured in previous studies, as the light transmissivity is determined by snow depth and ice thickness which vary widely, the under-ice light values presented in this study (0 – 193, $\bar{X} = 35$ µmol photons $m^{-2}s^{-1}$) were primarily within the expected spring range in high latitudes for the observed sea ice and snow conditions (Campbell et al., 2016; Leu et al., 2010). The few unusually high values (> 100 µmol photons $m^{-2}s^{-1}$) recorded were taken at sites with snow depth < 5 cm and ice thickness < 50 cm.

Under-ice light transmittance, as a function of ice thickness and snow depth, was related with the sea ice microalgal community composition. We found under-ice light transmittance to have a stronger association with community composition than other environmental variables, including temperature, ice salinity, brine volume and under-ice water nutrient concentration. Whilst initial community composition may play a role in determining the composition throughout the season, it was not able to be quantitatively evaluated as not all sampling sites were revisited throughout the season. The association between under-ice light and community composition was particularly evident during the early-mid growth season. In April, the communities exposed to higher under-ice light conditions were typically more diverse, with higher relative abundance of common ice-associated taxa such as *Navicula* spp., *C. closterium* and *Fragilariopsis* spp. This may reflect that increased light transmitted to the bottom ice, until a threshold, drives an increased growth rate in many bottom ice taxa (Hegseth, 1992). Similar patterns of enhanced diversity with increased under-ice light transmittance have been observed previously in both the Arctic Ocean (Hop et al., 2020) and the Barents Sea (Hegseth & von Quillfeldt, 2022).

One of the most prevalent species throughout our study was *N. frigida*, a species endemic to sea ice communities. This species has been found to form vast blooms throughout the Arctic (Hegseth & von

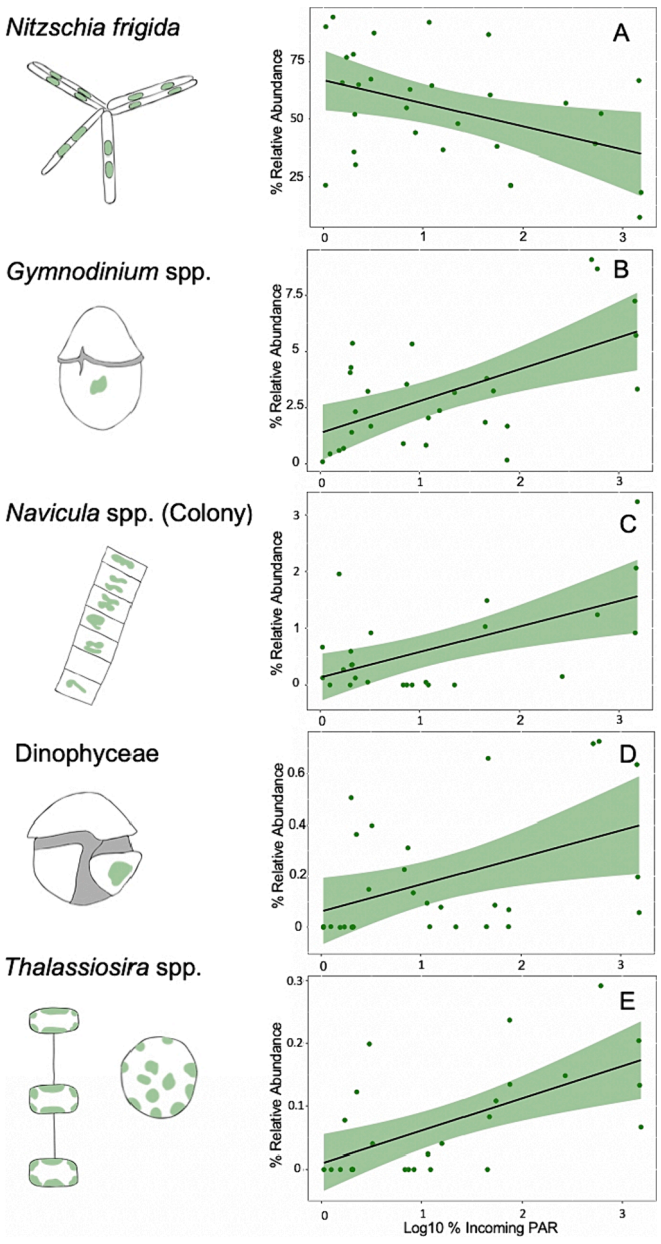

Fig. 5. Significant relationships for species-specific relative contribution to community composition vs. Log10 percent (%) incoming PAR during April and May, (A) *Nitzschia frigida*, (B) *Gymnodinium* spp., (C) Colony forming *Navicula* spp., (D) Dinophyceae and (E) *Thalassiosira* spp.. Data are fitted using linear regression with 95% confidence intervals (shading).

Quillfeldt, 2022; Hop et al., 2020). The relative abundance of *N. frigida* was negatively correlated with light and strongly associated with increased chl *a* concentration. These relationships were reflected in the onset of *N. frigida* blooms observed as the season progressed, coinciding with a reduction in under-ice light transmissivity, due to unusually high snow fall in the late spring (Norwegian Meteorological Institute, 2023). By early May, *N. frigida* dominated the communities at all sites, resulting in reduced overall diversity. This dominance by *N. frigida* during May could explain why no relationship was observed between under-ice light and diversity in May, and possibly indicates that light has a less distinct effect on the diversity of more established ice algal communities. When a higher proportion of incoming light was transmitted under the ice, a higher abundance of Dinophyceae overall was found (Fig. 5), yet a contrasting temporal effect was also detected, with a relative increase in abundance during seasonal progression despite lower light transmission. This suggests that it was the lower nitrate concentrations later in the season, evidenced by the elevated $\delta^{15}N$, that favoured the Dinophyceae, potentially having a greater influence on their proliferation than light. This increase in Dinophyceae dominance with seasonal progression is consistent with the patterns suggested by other studies (Alou-Font et al., 2013; Hegseth & von Quillfeldt, 2022; Rozanska et al., 2009) and such seasonal successions in taxa are seen across a range of systems (e.g. (McMinn & Hodgson, 1993; Winder & Varpe, 2020).

Concomitant with influencing the community composition, light transmissivity was positively correlated with $\delta^{13}C$ enrichment and increased C:N, mirroring previous work (Gosselin et al., 1990; Lee et al., 2008a), and demonstrating how light directly affects the biochemical composition of ice algae. The $\delta^{13}C$ values and C:N ratios within sea ice have been documented to range from -27 to -11‰ (Leu et al., 2020; Pineault et al., 2013), and 3 to 24 mols (Niemi & Michel, 2015), respectively, and our results are in line with these findings. Interestingly, we found no correlation between $\delta^{13}C$ content and protist abundance or chl *a*, unlike the positive correlations observed previously (Gradinger, 2009; Pineault et al., 2013). In dense sea ice assemblages which are highly productive and space limited, we expected to find enriched $\delta^{13}C$ values due to preferential assimilation of ^{12}C and minimal replenishment to the inorganic carbon pool (Pineault et al., 2013), so the lack of relationships between $\delta^{13}C$ with either protist abundance or chl *a* within this study, could potentially be explained by the relatively low biomass accumulated at the sites. Whilst the chl *a* concentrations are within the expected range for Arctic land-fast ice, they are on the lower end and do not represent a dense bloom scenario (Campbell et al., 2016; Leu et al., 2020; Runge, 2021). In addition, the relationship between stochiometric C:N ratios and under-ice light only, coupled with the fact that C:N ratios were typically at the Redfield Ratio of 6.6 or below, validates the greater influence of light than nutrient limitation at most sites (Campbell et al., 2016; Gosselin et al., 1990). On the other hand, $\delta^{15}N$ levels decreased with increasing protist abundance and were inversely related to the abundance of all taxa, particularly *N. frigida*. This relationship was not observed previously (Pineault et al., 2013). The observed decline in $\delta^{15}N$ levels could suggest an increase in nutrient recycling, relative abundance of autotrophs or dissolved inorganic nitrogen reduction (Pineault et al., 2013) with higher algal density, thus the $\delta^{15}N$ levels were not necessarily linked to under-ice light.

Based on the water column nutrient concentrations, the sites sampled were not nutrient limited, which differs from previous observations from late in the bottom ice algal season (Leu et al., 2020). This may be due to relatively low biomass accumulation at all sites, leaving a reservoir of unused nutrients. However, absolute values of nutrients within the sea ice algal boundary layer were not obtained and therefore, we cannot say with certainty that the microalgal cells were not experiencing some level of nutrient stress. That said, the assemblages in Tempelfjorden in late April and VM-5 (the outermost site in VM) in mid-late May were experiencing enriched $\delta^{13}C$ values between -14 and -17‰ and C:N ratios of >10, similar to those observed at high under-ice light sites in Van Mijenfjorden previously (Leu et al., 2020). Whilst it is possible that these sites were experiencing the onset of nutrient depletion within the ice, the under-water $NO_3^- + NO_2$ concentrations were still replete at all sites with values >1.5 μM. Rather than depletion of nitrate, it is possible that high light conditions could have resulted in a skewed uptake of C through the accumulation of C-rich storage compounds (Søreide et al., 2006), which can have significant consequences for transfer of energy through the marine food web (Hessen et al., 2008).

The unique community composition found at the TF-1 site (closest to the ice-edge) was unexpected and possibly a result of the site experiencing melting of the ice at the ice-ocean interface. It was characterised by high under-ice light (>100 μmol photons $m^{-2}s^{-1}$), low brine salinity, low chl *a* concentrations and seawater temperatures of -1.6 °C. These conditions may explain why the dominant species was *Entomoneis* spp, a large cryobenthic diatom which has been shown to perform well in low salinity melt conditions (Ryan et al., 2004). It is important to note that

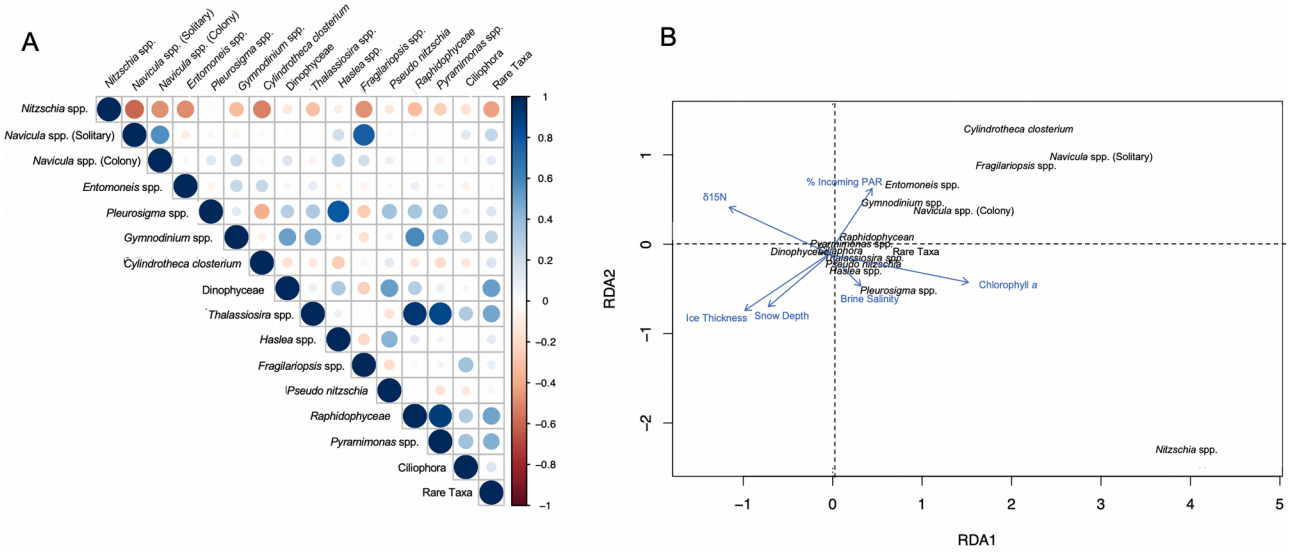

Fig. 6. (A) Correlation matrix of the relative abundance of main taxonomic groups found throughout April and May 2021, in land-fast ice, Svalbard, Norway. The strength of the positive (blue) and negative (red) correlations is displayed according to dot size. (B) Redundancy analysis (RDA) biplot of the relative abundance of taxonomic groups with environmental variables. Only significant vectors are shown.

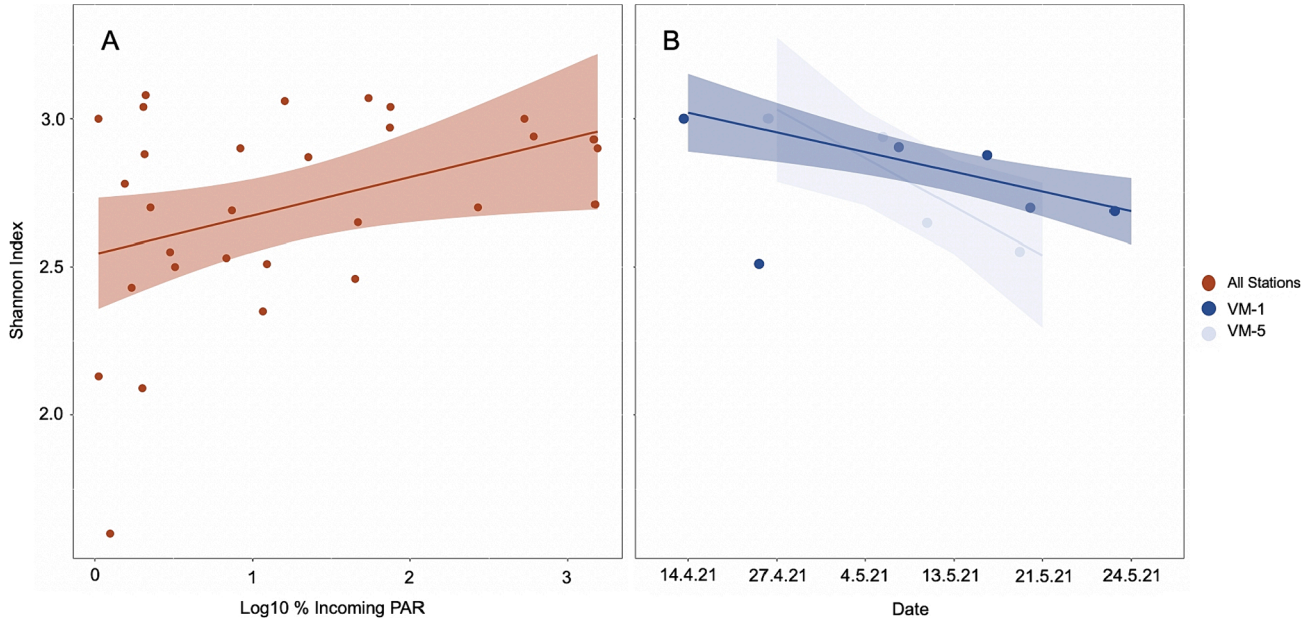

Fig. 7. Spatial and temporal microalgal diversity dynamics (A) in relation to Log10 percent (%) incoming PAR for all data and (B) as a function of time for the outermost (VM-5) (light blue) and innermost (VM-1) (dark blue) sites within Van Mijenfjorden. Data are fitted using linear regression with 95% confidence intervals (shading). The outlier on 27th April has been excluded from the regression within the VM-1 site data.

when considering all sampling sites, *Entomoneis* spp. was not correlated to brine salinity, however another large solitary diatom, *Pleurosigma* spp., was positively correlated with brine salinity, thus brine salinity is unlikely to be the only driver of relatively high abundance of *Entomoneis* spp. at TF-1. A unique community composition was also observed in the assemblage at TF-2, with high relative abundance of *C. closterium,* however it did not appear to be melting out as the site had higher brine salinity and lower under ice water temperatures of -1.8°C. Thus, based on the RDA it is likely that this assemblage is explained primarily by high light transmissivity (22% incoming PAR).

Previous studies have shown that the composition of the ice algal community can affect sympagic-pelagic-benthic coupling, as the melt community may seed the pelagic ecosystem, shaping the ensuing phytoplankton blooms (Jin et al., 2016; Michel et al., 1993; Pineault et al., 2013). An ice community dominated by colonial taxa forming aggregates has been shown to shift the dominance of the pelagic community from diatom to flagellate dominated, as the ice-associated aggregates of diatoms sink rapidly to the ocean floor (Tedesco et al., 2012). In addition, in the early season when grazing pressure in the pelagic zone is minimal, ice algae sinking to the ocean floor is an important food source for the benthos (McMahon et al., 2006) which may persist year round (Koch et al., 2023). Combined, these processes influence which taxa and nutrients are available to be transferred through trophic levels via pelagic and benthic pathways. The low $\delta^{13}C$ values observed in the water column indicate that the ice-associated algae had not yet made a quantitatively significant contribution to the pelagic community, likely

due to timing and the temperature of the ice, as most communities had not reached the end of season melt (i.e. under water ice temperatures remained at < -1.8°C, with some exceptions) and generally low light levels reaching the water column (i.e. 19 of 30 sites experienced < 20 μmol photons $m^{-2}s^{-1}$).

The strong links between the availability of ice algae and reproduction in some zooplankton species reinforces the importance of ice algae to the extent of secondary production and nutrition supplied to the marine food web, with estimates of the carbon contribution derived from sea ice algae to some zooplankton species being as high as 60% (Runge & Ingram, 1988; Søreide et al., 2013; Søreide et al., 2006). For example, reproduction in *Calanus glacialis* has been shown to begin under the sea ice, prior to the pelagic blooms, with availability of ice algae for grazing bringing forward oogenesis and oocyte maturation (Durbin & Casas, 2014). Ice algae availability can also boost fecundity, as the population reach higher numbers when the first feeding naupliar stage aligns with the subsequent pelagic phytoplankton bloom (Ringuette et al., 2002; Søreide et al., 2010) and it has been proposed that a longer ice-covered season could result in a longer spawning season and larger cohort for *C. glacialis* (Durbin & Casas, 2014). Copepods have also been observed to preferentially consume ice algae over pelagic phytoplankton during the reproductive period (Durbin & Casas, 2014). This is likely due to a preference for cells containing higher lipid content, such as has often been measured in sea ice algae at the end of the spring season (Lee et al., 2008b; Smith et al., 1993).

The rapidly declining expanse and duration of land-fast ice in the Arctic means that communities reliant on this icy habitat are experiencing an ecosystem in flux, where snow and ice thickness are likely to vary across space and time. The implications of this instability will be highly variable light transmissivity, which in turn alters ice algal community composition, and thus likely the sea ice and pelagic primary and secondary production, as well as benthic productivity (Currie et al., 2021). Under a future scenario of warmer water and air temperatures, Arctic sea ice and snow depth are projected to be thinner (Kacimi & Kwok, 2022; Renner et al., 2014; Webster et al., 2014), thereby permitting greater light transmittance through the ice. Whilst our findings are constrained to correlative relationships, if our data are indicative of broader Arctic bottom ice communities, then these data suggest that a higher light under-ice environment could reshape the bottom ice algal communities towards higher diversity, with a greater contribution of dinoflagellates. Any shift away from diatoms and towards dinoflagellates would have trophic and biogeochemical implications, influencing both the transfer of energy through the food web and oceanic mineral cycling. For example, copepods and especially *Calanus* spp., the dominant zooplankton in Arctic waters, have a strong reliance on carbon derived from a diatom-based diet (Søreide et al., 2008). A reduced relative contribution of diatoms and a higher relative abundance of dinoflagellates would affect the fatty acid content available to higher trophic levels, as diatoms are high in C16 PUFA, essential fatty acids (20:5n-3) and omega-7 fatty acids (16:1n-7), whilst dinoflagellates are high in C18 and C22 PUFA (Dalsgaard et al., 2003). In addition, a shift to a dinoflagellate dominated community would alter ocean biogeochemistry, as diatoms have a unique siliceous cell structure that acts as ballast, making them effective at exporting carbon to ocean depths and key players in biogenic silicon cycling (Baines et al., 2010). That said, the high, late-season snowfall observed during this study meant that light transmissivity declined as time progressed, highlighting how the stochasticity of snow fall adds a layer of complexity to the seasonality of light (which generally increases with the onset of Arctic summer). As lower light transmissivity correlated with a less diverse ice algal community, depending on the dominating taxa, this too would influence carbon transfer through the food web. A community dominated by colonial species such as *N. frigida*, or larger solitary species such as *Pleurosigma* spp. or *Entomoneis* spp., affects grazing efficiency in smaller copepod species, whereas smaller algal taxa reduce grazing efficiency in larger copepod species (Levinsen et al., 2000). Such a shift has been observed in the Antarctic krill *Euphasia superba*, which showed only 50% grazing efficiency for phytoplankton < 20 μm (Boyd et al., 1984). Given the potential for higher precipitation (snowfall) to occur in the Arctic in the short-medium term (Liu et al., 2012; van Pelt et al., 2016), which would invariably reduce light transmittance to under ice communities (Perovich, 2007), we may see ice algal communities that are less diverse. Should the increased precipitation come as rain however, which is increasing in parts of the Arctic (Hansen et al., 2014), the snow cover would be reduced and the light transmittance would increase, potentially resulting in a more diverse ice algae community, as described above. Such conditions would also likely limit ice algae community establishment and biomass due to bottom ablation (Juhl & Krembs, 2010). While continuing and rapid environmental change is an established component of global warming, due to the many complexities of interactions and feedback mechanisms, the direction of the change is less decided.

This seasonal study has offered a unique insight into algal community composition in Arctic land-fast sea ice across broad temporal and spatial scales and examined the relationship between the community structure and environmental variables with a particular focus on the under-ice light environment. We showed that the bottom ice community composition was strongly correlated with under-ice light transmissivity, with algal assemblages generally exhibiting greater species diversity when experiencing more light early in the productive season. These findings are important, because shifts in ice algal community composition can have both trophic effects through changes to size and food quality, and biogeochemical implications. Furthermore, these data intimate that the tight coupling between ice algae abundance and zooplankton success would be affected by alterations to sea ice thickness and snow cover, with the precise direction of change being interwoven with the extent and direction of environmental change. Through revealing the importance of light availability on shaping Arctic land-fast ice algal communities, we have provided baseline data that can help inform predictive models to better constrain the ecological impacts of environmental change to polar marine food webs, which depend on these ice-based organisms.

CRediT authorship contribution statement

Rebecca J. Duncan: Conceptualization, Methodology, Formal analysis, Investigation, Data curation, Writing – original draft, Visualization, Funding acquisition. **Janne E. Søreide:** Conceptualization, Data curation, Funding acquisition, Methodology, Resources, Supervision, Writing – review & editing. **Øystein Varpe:** Conceptualization, Methodology, Supervision, Writing – review & editing. **Józef Wiktor:** Supervision, Validation, Writing – review & editing. **Vanessa Pitusi:** Data curation, Investigation, Writing – review & editing. **Elaine Runge:** Investigation, Writing – review & editing. **Katherina Petrou:** Conceptualization, Methodology, Supervision, Writing – review & editing.

Declaration of competing interest

The authors declare that they have no known competing financial interests or personal relationships that could have appeared to influence the work reported in this paper.

Data availability

Data will be made available on request.

Acknowledgements

Duncan RJ is supported by an Australian Government Research Training Program Scholarship, an AINSE Ltd. Postgraduate Research Award (PGRA) and an Arctic Field Grant (310664) provided by the Research Council of Norway (RCN). Runge E was also supported with an

Arctic Field Grant (310692). Further, funding was provided through the 2017-2018 Belmont Forum and BiodivERsA joint call for research proposals, under the BiodivScen ERA-Net COFUND programme, and with the funding organisations RCN (296836) and National Science Centre Poland (UMO-2015/17/B/NZ8/02473)

Appendix A. Supplementary data

Supplementary data to this article can be found online at https://doi.org/10.1016/j.pocean.2024.103248.

References

Allaart, L., Müller, J., Schomacker, A., Rydningen, T.A., Håkansson, L., Kjellman, S.E., Mollenhauer, G., Forwick, M., 2020. Late Quaternary glacier and sea-ice history of northern Wijdefjorden, Svalbard. Boreas 49 (3), 417–437.

Alou-Font, E., Mundy, C.-J., Roy, S., Gosselin, M., Agustí, S., 2013. Snow cover affects ice algal pigment composition in the coastal Arctic Ocean during spring. Mar. Ecol. Prog. Ser. 474, 89–104.

Archer, S.D., Leakey, R.J., Burkill, P.H., Sleigh, M.A., Appleby, C.J., 1996. Microbial ecology of sea ice at a coastal Antarctic site: community composition, biomass and temporal change. Mar. Ecol. Prog. Ser. 135, 179–195.

Arrigo, K.R., 2014. Sea ice ecosystems. Ann. Rev. Mar. Sci. 6, 439–467.

Baines, S.B., Twining, B.S., Brzezinski, M.A., Nelson, D.M., Fisher, N.S., 2010. Causes and biogeochemical implications of regional differences in silicification of marine diatoms. Global Biogeochem. Cycles 24 (4), GB4031.

Barrie, A., Davies, J., Park, A., Workman, C., 1989. Continuous-flow stable isotope analysis for biologists. Spectroscopy 4 (7), 42–52.

Berggreen, U., Hansen, B., Kiørboe, T., 1988. Food size spectra, ingestion and growth of the copepodAcartia tonsa during development: Implications for determination of copepod production. Mar. Biol. 99 (3), 341–352.

Boetius, A., Albrecht, S., Bakker, K., Bienhold, C., Felden, J., Fernández-Méndez, M., Hendricks, S., Katlein, C., Lalande, C., Krumpen, T., 2013. Export of algal biomass from the melting Arctic sea ice. Science 339 (6126), 1430–1432.

Boyd, C.M., Heyraud, M., Boyd, C.N., 1984. Feeding of the Antarctic krill *Euphausia superba*. J. Crustac. Biol. 4 (5), 123–141.

Campbell, K., Mundy, C., Landy, J., Delaforge, A., Michel, C., Rysgaard, S., 2016. Community dynamics of bottom-ice algae in Dease Strait of the Canadian Arctic. Prog. Oceanogr. 149, 27–39.

Campbell, K., Mundy, C., Belzile, C., Delaforge, A., Rysgaard, S., 2018. Seasonal dynamics of algal and bacterial communities in Arctic sea ice under variable snow cover. Polar Biol. 41 (1), 41–58.

Campbell, K., Mundy, C., Juhl, A.R., Dalman, L.A., Michel, C., Galley, R.J., Else, B.E., Geilfus, N.X., Rysgaard, S., 2019. Melt procedure affects the photosynthetic response of sea ice algae. Front. Earth Sci. 7, 21.

Comeau, A.M., Philippe, B., Thaler, M., Gosselin, M., Poulin, M., Lovejoy, C., 2013. Protists in Arctic drift and land-fast sea ice. J. Phycol. 49 (2), 229–240.

Connan-McGinty, S., Banas, N.S., Berge, J., Cottier, F., Grant, S., Johnsen, G., Kopec, T. P., Porter, M., McKee, D., 2022. Midnight sun to Polar Night: A model of seasonal light in the Barents Sea. J. Adv. Model. Earth Syst. 14 (10), e2022MS003198.

Cota, G., Legendre, L., Gosselin, M., Ingram, R., 1991. Ecology of bottom ice algae: I. Environmental controls and variability. J. Mar. Syst. 2 (3–4), 257–277.

Cox, G.F., Weeks, W.F., 1983. Equations for determining the gas and brine volumes in sea-ice samples. J. Glaciol. 29 (102), 306–316.

Currie, A.A., Marshall, A.J., Lohrer, A.M., Cummings, V.J., Seabrook, S., Cary, S.C., 2021. Sea ice dynamics drive benthic microbial communities in McMurdo Sound. Antarctica. *Frontiers in Microbiology* 12, 745915.

Dalsgaard, J., John, M.S., Kattner, G., Müller-Navarra, D., Hagen, W., 2003. Fatty acid trophic markers in the pelagic marine environment. Adv. Mar. Biol 46, 226–340.

Duncan, R.J., Nielsen, D., Søreide, J.E., Varpe, Ø., Tobin, M.J., Pitusi, V., Heraud, P., Petrou, K., 2024. Biomolecular profiles of Arctic Sea-ice diatoms highlight the role of under-ice light in cellular energy allocation. ISME Commun. 4 (1), 1–15.

Duncan, R.J., Nielsen, D.A., Sheehan, C.E., Deppeler, S., Hancock, A.M., Schulz, K.G., Davidson, A.T., Petrou, K., 2022. Ocean acidification alters the nutritional value of Antarctic diatoms. New Phytol. 233 (4), 1813–1827.

Durbin, E.G., Casas, M.C., 2014. Early reproduction by *Calanus glacialis* in the Northern Bering Sea: the role of ice algae as revealed by molecular analysis. J. Plankton Res. 36 (2), 523–541.

Edler, L., Elbrächter, M., 2010. The Utermöhl method for quantitative phytoplankton analysis. In: Karlson, B. (Ed.), Microscopic and Molecular Methods for Quantitative Phytoplankton Analysis. United Nations Educational, Scientific and Cultural Organization (UNESCO), Paris, pp. 13–20.

Fernández-Méndez, M., Katlein, C., Rabe, B., Nicolaus, M., Peeken, I., Bakker, K., Flores, H., Boetius, A., 2015. Photosynthetic production in the central Arctic Ocean during the record sea-ice minimum in 2012. Biogeosciences 12 (11), 3525–3549.

Forwick, M., Vorren, T.O., Hald, M., Korsun, S., Roh, Y., Vogt, C., Yoo, K.-C., 2010. Spatial and temporal influence of glaciers and rivers on the sedimentary environment in Sassenfjorden and Tempelfjorden, Spitsbergen. Geol. Soc. Lond. Spec. Publ. 344 (1), 163–193.

Gosselin, M., Legendre, L., Therriault, J.C., Demers, S., 1990. Light and nutrient limitation of sea-ice microalgae (Hudson Bay, Canadian Arctic). J. Phycol. 26 (2), 220–232.

Gosselin, M., Levasseur, M., Wheeler, P.A., Horner, R.A., Booth, B.C., 1997. New measurements of phytoplankton and ice algal production in the Arctic Ocean. Deep Sea Res. Part II 44 (8), 1623–1644.

Gradinger, R., 2009. Sea-ice algae: Major contributors to primary production and algal biomass in the Chukchi and Beaufort Seas during May/June 2002. Deep Sea Res. Part II 56 (17), 1201–1212.

Haarpaintner, J., Haugan, P.M., Gascard, J.-C., 2001. Interannual variability of the Storfjorden (Svalbard) ice cover and ice production observed by ERS-2 SAR. Ann. Glaciol. 33, 430–436.

Hansen, B.B., Isaksen, K., Benestad, R.E., Kohler, J., Pedersen, Å.Ø., Loe, L.E., Coulson, S. J., Larsen, J.O., Varpe, Ø., 2014. Warmer and wetter winters: characteristics and implications of an extreme weather event in the High Arctic. Environ. Res. Lett. 9 (11), 114021.

Hegseth, E.N., 1992. Sub-ice algal assemblages of the Barents Sea: species composition, chemical composition, and growth rates. Polar Biol. 12, 485–496.

Hegseth, E.N., von Quillfeldt, C., 2022. The Sub-Ice Algal Communities of the Barents Sea Pack Ice: Temporal and Spatial Distribution of Biomass and Species. Journal of Marine Science and Engineering 10 (2), 164.

Hessen, D.O., Leu, E., Færøvig, P.J., Petersen, S.F., 2008. Light and spectral properties as determinants of C: N: P-ratios in phytoplankton. Deep Sea Res. Part II 55 (20–21), 2169–2175.

Hitchcock, G.L., 1982. A comparative study of the size-dependent organic composition of marine diatoms and dinoflagellates. J. Plankton Res. 4 (2), 363–377.

Holm-Hansen, O., Riemann, B., 1978. Chlorophyll a determination: improvements in methodology. Oikos 30, 438–447.

Hop, H., Vihtakari, M., Bluhm, B.A., Assmy, P., Poulin, M., Gradinger, R., Peeken, I., von Quillfeldt, C., Olsen, L.M., Zhitina, L., 2020. Changes in sea-ice protist diversity with declining sea ice in the Arctic Ocean from the 1980s to 2010s. Front. Mar. Sci. 7, 243.

Horner, R. (Ed.), 1985. Sea Ice Biota, 1st edition ed. CRC Press, Boca Raton, USA.

Høyland, K.V., 2009. Ice thickness, growth and salinity in Van Mijenfjorden, Svalbard. Norway. *Polar Research* 28 (3), 339–352.

Institute, N.M., 2023. Svalbard LH Meterological Station Snow Depth. Retrieved 24.9.23 from Norwegian Meteorological Institute. https://www.yr.no/en/statistics/graph/5-99840/Norway/Svalbard/Svalbard/Svalbard%20LH?q=2021.

Ji, R., Jin, M., Varpe, Ø., 2013. Sea ice phenology and timing of primary production pulses in the Arctic Ocean. Glob. Chang. Biol. 19 (3), 734–741.

Jin, M., Popova, E.E., Zhang, J., Ji, R., Pendleton, D., Varpe, Ø., Yool, A., Lee, Y.J., 2016. Ecosystem model intercomparison of under-ice and total primary production in the Arctic Ocean. J. Geophys. Res. Oceans 121 (1), 934–948.

Juhl, A.R., Krembs, C., 2010. Effects of snow removal and algal photoacclimation on growth and export of ice algae. Polar Biol. 33, 1057–1065.

Kacimi, S., Kwok, R., 2022. Arctic Snow Depth, Ice Thickness, and Volume From ICESat-2 and CryoSat-2: 2018–2021. Geophys. Res. Lett. 49 (5), e2021GL097448.

Koch, C.W., Brown, T.A., Amiraux, R., Ruiz-Gonzalez, C., MacCorquodale, M., Yunda-Guarin, G.A., Kohlbach, D., Loseto, L.L., Rosenberg, B., Hussey, N.E., 2023. Year-round utilization of sea ice-associated carbon in Arctic ecosystems. Nat. Commun. 14 (1), 1964.

Kunisch, E., Graeve, M., Gradinger, R., Haug, T., Kovacs, K.M., Lydersen, C., Varpe, Ø., Bluhm, B., 2021. Ice-algal carbon supports harp and ringed seal diets in the European Arctic: evidence from fatty acid and stable isotope markers. Mar. Ecol. Prog. Ser. 675, 181–197.

Kvernvik, A.C., Hoppe, C.J.M., Greenacre, M., Verbiest, S., Wiktor, J.M., Gabrielsen, T. M., Reigstad, M., Leu, E., 2021. Arctic sea ice algae differ markedly from phytoplankton in their ecophysiological characteristics. Mar. Ecol. Prog. Ser. 666, 31–55.

Lee, S.H., Whitledge, T.E., Kang, S.-H., 2008a. Carbon uptake rates of sea ice algae and phytoplankton under different light intensities in a landfast sea ice zone, Barrow, Alaska. *Arctic* 61 (3), 281–291.

Lee, S.H., Whitledge, T.E., Kang, S.-H., 2008b. Spring time production of bottom ice algae in the landfast sea ice zone at Barrow, Alaska. J. Exp. Mar. Biol. Ecol. 367 (2), 204–212.

Leu, E., Wiktor, J., Søreide, J., Berge, J., Falk-Petersen, S., 2010. Increased irradiance reduces food quality of sea ice algae. Mar. Ecol. Prog. Ser. 411, 49–60.

Leu, E., Søreide, J., Hessen, D., Falk-Petersen, S., Berge, J., 2011. Consequences of changing sea-ice cover for primary and secondary producers in the European Arctic shelf seas: timing, quantity, and quality. Prog. Oceanogr. 90 (1–4), 18–32.

Leu, E., Brown, T.A., Graeve, M., Wiktor, J., Hoppe, C.J., Chierici, M., Fransson, A., Verbiest, S., Kvernvik, A.C., Greenacre, M.J., 2020. Spatial and temporal variability of ice algal trophic markers—with recommendations about their application. Journal of Marine Science and Engineering 8 (9), 676.

Levinsen, H., Turner, J.T., Nielsen, T.G., Hansen, B.W., 2000. On the trophic coupling between protists and copepods in arctic marine ecosystems. Mar. Ecol. Prog. Ser. 204, 65–77.

Li, Z., Zhao, J., Su, J., Li, C., Cheng, B., Hui, F., Yang, Q., Shi, L., 2019. Spatial and temporal variations in the extent and thickness of arctic landfast ice. Remote Sens. 12 (1), 64.

Liu, J., Curry, J.A., Wang, H., Song, M., Horton, R.M., 2012. Impact of declining Arctic sea ice on winter snowfall. PNAS 109 (11), 4074–4079.

McMahon, K.W., Ambrose Jr, W.G., Johnson, B.J., Sun, M.-Y., Lopez, G.R., Clough, L.M., Carroll, M.L., 2006. Benthic community response to ice algae and phytoplankton in Ny Ålesund, Svalbard. Mar. Ecol. Prog. Ser. 310, 1–14.

McMinn, A., Hodgson, D., 1993. Summer phytoplankton succession in Ellis Fjord, eastern Antarctica. J. Plankton Res. 15 (8), 925–938.

Michel, C., Legendre, L., Therriault, J.-C., Demers, S., Vandevelde, T., 1993. Springtime coupling between ice algal and phytoplankton assemblages in southeastern Hudson Bay. Canadian Arctic. *Polar Biology* 13 (7), 441–449.
Michel, C., Legendre, L., Ingram, R., Gosselin, M., Levasseur, M., 1996. Carbon budget of sea-ice algae in spring: Evidence of a significant transfer to zooplankton grazers. J. Geophys. Res. Oceans 101 (C8), 18345–18360.
Niemi, A., Michel, C., 2015. Temporal and spatial variability in sea-ice carbon: nitrogen ratios on canadian arctic shelvestemporal and spatial variability in sea-ice carbon: Nitrogen ratios. Elementa 3, 1–12.
Oksanen, J., Blanchet, F.G., Kindt, R., Legendre, P., Minchin, P.R., O'hara, R., Simpson, G.L., Solymos, P., Stevens, M.H.H., Wagner, H., 2013. Package 'vegan'. Community ecology package, version 2 (9), 1–295.
Palmisano, A.C., SooHoo, J.B., Sullivan, C.W., 1985. Photosynthesis-irradiance relationships in sea ice microalgae from mcmurdo sound, Antarctica. J. Phycol. 21 (3), 341–346.
Parsons, T.R., 2013. A manual of chemical & biological methods for seawater analysis. Elsevier, New York, USA.
Perovich, D.K., 1996. The optical properties of sea ice. U. S. Cold Reg. Res. and Eng. Lab. Monogr. 96–1.
Perovich, D.K., 2007. Light reflection and transmission by a temperate snow cover. J. Glaciol. 53 (181), 201–210.
Petrou, K., Ralph, P., 2011. Photosynthesis and net primary productivity in three Antarctic diatoms: possible significance for their distribution in the Antarctic marine ecosystem. Mar. Ecol. Prog. Ser. 437, 27–40.
Pfister, G., McKenzie, R., Liley, J., Thomas, A., Forgan, B., Long, C.N., 2003. Cloud coverage based on all-sky imaging and its impact on surface solar irradiance. J. Appl. Meteorol. Climatol. 42 (10), 1421–1434.
Pineault, S., Tremblay, J.É., Gosselin, M., Thomas, H., Shadwick, E., 2013. The isotopic signature of particulate organic C and N in bottom ice: Key influencing factors and applications for tracing the fate of ice-algae in the Arctic Ocean. J. Geophys. Res. Oceans 118 (1), 287–300.
Quetin, L., Ross, R., 1985. Feeding by Antarctic Krill, Euphausia superba: does size matter?. In: Antarctic Nutrient Cycles And Food Webs. Springer: Berlin/Heidelberg, Germany, pp. 372–377.
Ratkova, T.N., Wassmann, P., 2005. Sea ice algae in the White and Barents seas: composition and origin. Polar Res. 24 (1–2), 95–110.
Renner, A.H., Gerland, S., Haas, C., Spreen, G., Beckers, J.F., Hansen, E., Nicolaus, M., Goodwin, H., 2014. Evidence of Arctic sea ice thinning from direct observations. Geophys. Res. Lett. 41 (14), 5029–5036.
Riebesell, U., Schloss, I., Smetacek, V., 1991. Aggregation of algae released from melting sea ice: implications for seeding and sedimentation. Polar Biol. 11, 239–248.
Ringuette, M., Fortier, L., Fortier, M., Runge, J.A., Bélanger, S., Larouche, P., Weslawski, J.-M., Kwasniewski, S., 2002. Advanced recruitment and accelerated population development in Arctic calanoid copepods of the North Water. Deep Sea Res. Part II 49 (22–23), 5081–5099.
Rozanska, M., Gosselin, M., Poulin, M., Wiktor, J., Michel, C., 2009. Influence of environmental factors on the development of bottom ice protist communities during the winter–spring transition. Mar. Ecol. Prog. Ser. 386, 43–59.
Runge, J.A., Ingram, R.G., 1988. Underice grazing by planktonic, calanoid copepods in relation to a bloom of ice microalgae in southeastern Hudson Bay. Limnol. Oceanogr. 33 (2), 280–286.
Runge, J., Ingram, R.G., 1991. Under-ice feeding and diel migration by the planktonic copepods Calanus glacialis and Pseudocalanus minutus in relation to the ice algal production cycle in southeastern Hudson Bay, Canada. Mar. Biol. 108, 217–225.
Runge, E. (2021). *Timing and magnitude of sea ice algal blooms in Svalbard archipelago: synthesis of chlorophyll a and driving physical environmental variables from 2007 to 2021* [Master Thesis, University of Copenhagen].
Ryan, K., Ralph, P., McMinn, A., 2004. Acclimation of Antarctic bottom-ice algal communities to lowered salinities during melting. Polar Biol. 27 (11), 679–686.
Ryan, K., Tay, M., Martin, A., McMinn, A., Davy, S., 2011. Chlorophyll fluorescence imaging analysis of the responses of Antarctic bottom-ice algae to light and salinity during melting. J. Exp. Mar. Biol. Ecol. 399 (2), 156–161.
Sackett, O., Petrou, K., Reedy, B., De Grazia, A., Hill, R., Doblin, M., Beardall, J., Ralph, P., Heraud, P., 2013. Phenotypic plasticity of southern ocean diatoms: key to success in the sea ice habitat? PLoS One 8 (11), e81185.
Shapiro, S.S., Wilk, M.B., 1965. An analysis of variance test for normality (complete samples). Biometrika 52 (3/4), 591–611.
Smith, R., Anning, J., Pierre Clement, G., 1988. Abundance and production of ice algae in Resolute Passage, Canadian Arctic. Mar. Ecol. Prog. Ser. 48, 251–263.
Smith, R.E., Cavaletto, J.F., Eadie, B., Gardner, W.S., 1993. Growth and lipid composition of high Arctic ice algae during the spring bloom at Resolute, Northwest Territories, Canada. Mar. Ecol. Prog. Ser. 97 (1), 19–29.
Somerfield, P.J., Clarke, K.R., Gorley, R.N., 2021. Analysis of similarities (ANOSIM) for 2-way layouts using a generalised ANOSIM statistic, with comparative notes on Permutational Multivariate Analysis of Variance (PERMANOVA). Austral Ecol. 46 (6), 911–926.
Søreide, J.E., Hop, H., Carroll, M.L., Falk-Petersen, S., Hegseth, E.N., 2006. Seasonal food web structures and sympagic–pelagic coupling in the European Arctic revealed by stable isotopes and a two-source food web model. Prog. Oceanogr. 71 (1), 59–87.
Søreide, J.E., Falk-Petersen, S., Hegseth, E.N., Hop, H., Carroll, M.L., Hobson, K.A., Blachowiak-Samolyk, K., 2008. Seasonal feeding strategies of Calanus in the high-Arctic Svalbard region. Deep Sea Res. Part II 55 (20–21), 2225–2244.
Søreide, J.E., Leu, E.V., Berge, J., Graeve, M., Falk-Petersen, S., 2010. Timing of blooms, algal food quality and *Calanus glacialis* reproduction and growth in a changing Arctic. Glob. Chang. Biol. 16 (11), 3154–3163.
Søreide, J.E., Carroll, M.L., Hop, H., Ambrose Jr, W.G., Hegseth, E.N., Falk-Petersen, S., 2013. Sympagic-pelagic-benthic coupling in Arctic and Atlantic waters around Svalbard revealed by stable isotopic and fatty acid tracers. Mar. Biol. Res. 9 (9), 831–850.
Søreide, J.E., Dmoch, K., Blachowiak-Samolyk, K., Trudnowska, E., Daase, M., 2022. Seasonal mesozooplankton patterns and timing of life history events in high-arctic fjord environments. Front. Mar. Sci. 9, 1–19.
Tedesco, L., Vichi, M., Thomas, D.N., 2012. Process studies on the ecological coupling between sea ice algae and phytoplankton. Ecol. Model. 226, 120–138.
Tomas, C.R., 1997. Identifying marine phytoplankton. Academic Press: San Diego, USA.
Urbański, J.A., Litwicka, D., 2022. The decline of Svalbard land-fast sea ice extent as a result of climate change. Oceanologia 64 (3), 535–545.
van Pelt, W.J., Kohler, J., Liston, G., Hagen, J.O., Luks, B., Reijmer, C., Pohjola, V.A., 2016. Multidecadal climate and seasonal snow conditions in Svalbard. J. Geophys. Res. Earth Surf. 121 (11), 2100–2117.
Varpe, Ø., Daase, M., Kristiansen, T., 2015. A fish-eye view on the new Arctic lightscape. ICES J. Mar. Sci. 72 (9), 2532–2538.
Vonnahme, T., 2021. Microbial diversity and ecology in the coastal Arctic seasonal ice zone.[Doctoral Dissertation, University in Tromsø].
Webster, M.A., Rigor, I.G., Nghiem, S.V., Kurtz, N.T., Farrell, S.L., Perovich, D.K., Sturm, M., 2014. Interdecadal changes in snow depth on Arctic sea ice. J. Geophys. Res. Oceans 119 (8), 5395–5406.
Wickham, H., Chang, W., Wickham, M.H., 2016. Package 'ggplot2'. *Create elegant data visualisations using the grammar of graphics*. Version 2 (1), 1–189.
Wickham, H., Averick, M., Bryan, J., Chang, W., McGowan, L.D.A., François, R., Grolemund, G., Hayes, A., Henry, L., Hester, J., 2019. Welcome to the Tidyverse. Journal of Open Source Software 4 (43), 1686.
Wiktor, J., Okolodkov, J., Vinogradova, K., 1995. *Atlas of the Marine Flora of Southern Spitsbergen*. Polish Academy of Sciences Institute, Gdansk, Poland.
Winder, M., Varpe, Ø., 2020. Interactions in plankton food webs: seasonal succession and phenology of Baltic Sea zooplankton. In: *Zooplankton Ecology*. CRC Press Taylor & Francis Group, Boca Raton, USA, pp. 162–191.
Yu, Y., Stern, H., Fowler, C., Fetterer, F., Maslanik, J., 2014. Interannual variability of Arctic landfast ice between 1976 and 2007. J. Clim. 27 (1), 227–243.